Homeopathy (2016) 105, 109–118
© 2015 The Faculty of Homeopathy. Published by Elsevier Ltd. All rights reserved.
http://dx.doi.org/10.1016/j.homp.2015.08.007, available online at http://www.sciencedirect.com

ORIGINAL PAPER

Inhalation therapy with M1 inhibits experimental melanoma development and metastases in mice

Lucas Ferrari de Andrade[1], Brian Mozeleski[2], Aline Raquell Leck[1], Gustavo Rossi[1], Cleber Rafael Vieira da Costa[1], Fernando de Souza Fonseca Guimarães[3], Rafael Zotz[4], Katia Fialho do Nascimento[1], Carolina Camargo de Oliveira[1], Dorly de Freitas Buchi[1] and Edvaldo da Silva Trindade[1,*]

[1]*Universidade Federal do Paraná, Setor de Ciências Biológicas, Departamento de Biologia Celular, Laboratório de Células Inflamatórias e Neoplásicas, Coronel Francisco Heráclito dos Santos, Curitiba, PR, 81530-900, Brazil*
[2]*Institut Pasteur, Unité de Régulation Immunitaire et Vaccinologie, Département d'Immunologie, 25-28 rue du Docteur Roux, 75724, Paris, France*
[3]*Queensland Institute of Medical Research, Immunology in Cancer and Infection, 300 Herston Rd, Brisbane, QLD, 4006, Australia*
[4]*Pontifícia Universidade Católica do Paraná, Biotério Central, 155, Imaculada Conceição, Bairro Prado Velho, Curitiba, PR, 80215-901, Brazil*

Background: **M1 is a homeopathic medicine with immunostimulatory properties used mainly by cancer patients to complement current therapies. Metastatic melanoma is a skin-originated form of cancer without a single therapy able to produce high rate and sustained responses, which attracts the use of complementary therapies such as M1. However, M1's anti-melanoma effects remain to be pre-clinically demonstrated. Therefore in the present work, we utilized a pulmonary metastatic melanoma model and a subcutaneous melanoma growth model to investigate the potential benefits of treatment with M1.**

Methods: **C57BL/6 mice were injected intravenously or subcutaneously with B16F10 mouse melanoma cells. After 24 h, mice were treated with either M1 or vehicle (water) for 14 days, euthanized and harvested for multi-parameter pulmonary and tumor analyses.**

Results: **Mice treated with M1 had significantly lower tumor burden in the lungs and subcutaneous tissue than control mice. Furthermore, tumors were impaired in proliferation and tumor related angiogenesis by the inhibition of myeloid derived suppressor cells (MDSC) positive for angiotensin II type 1 receptor (AT1R).**

Conclusion: **Altogether these data suggest M1 is an efficient candidate for melanoma therapy to be considered for future clinic studies as this study is the first supporting the idea that melanoma patients may benefit with the treatment. The treatment with M1 provides advantages considering the highly-diluted properties and a cost effective alternative to costly chemotherapeutic approaches with, if any, lower toxicity.** *Homeopathy* (2016) **105**, 109–118.

Keywords: Melanoma; Homeopathy; M1; Angiotensin II receptor; Angiogenesis; Tumor growth

*Correspondence: Edvaldo da Silva Trindade, Universidade Federal do Paraná, Setor de Ciências Biológicas, Departamento de Biologia Celular, Laboratório de Células Inflamatórias e Neoplásicas, Coronel Francisco Heráclito dos Santos, Curitiba, PR, 81530-900, Brazil.
E-mail: brian.mozeleski@gmail.com, fernando.guimaraes@qimrberghofer.edu.au, rafael.zotz@pucpr.br, labbiocel@ufpr.br
Received 19 August 2014; revised 17 July 2015; accepted 13 August 2015

Introduction

Despite major advances in cancer therapy, resulting in increased survival and cure rates, cancer remains the leading cause of death worldwide. The most recent World Health Organization (WHO) estimate indicated that 8.6 million (M) people died of cancer in 2012.[1] For example in the United States an estimated 1.6 M new cancer cases and 0.6 M cancer deaths are projected to occur in 2014. In addition, skin cancer incidence included estimates of 76,100 of new melanoma cases with 12.7% of mortality.[2] Melanoma, a skin cancer resulting in 75% of skin cancer related death, originates from melanocytes located on the basal membrane of the epithelium tissue.[3] Early identification and diagnosis of melanoma can be treated with high effectiveness, yet contrastingly, if melanoma metastasizes to distal organs the median overall survival can be a brief 8−18 months. These consequences place metastatic melanoma as the most aggressive and dangerous form of skin cancer.[4]

Melanoma drug discovery currently represents the majority of effort in combating this deadly disease. Considering the high immunogenicity of melanoma tumors, therapies aimed to modulate or disarm tumor evading mechanisms and subsequently stimulate proficient anti-tumor immune response have gained considerable focus as of late.[5–7] It has been previously administered extensive and successful studies in trials of different formulations of highly diluted medicines following homeopathic approaches.[8–11] Following high throughput screening, a homeopathic medicine termed 'M1' was the most successful candidate based on several parameters of immune responses mediated by $CD8^+$ T lymphocytes in mice lymph nodes.[12] This commercial medicine has been indicated by homeopathic doctors in Brazil to complement the therapy of patients with immunologic-related disorders, such as cancer. Despite many cancer patients claim to benefit from homeopathic treatments,[13] M1 was not investigated yet in pre-clinical studies for melanoma.

Given M1 effects in the immune system, we now aimed to investigate whether this treatment affects tumor development and metastases. We chose to study melanoma because is an important clinical issue. There is no practical alternative to animal experiments in this case, therefore we used a mouse model. We chose to study B16F10 melanoma, an aggressive mouse tumor that can be treated with immunotherapies.[14] This pre-clinical study presented here provides data supporting the efficacy of M1 for melanoma therapy. Using a method based on combinatory and high occurrence rates and low doses of M1 inhaled, as previously described,[15] we show for the first time that M1 treatment reduced the tumor burden of an experimental pulmonary metastasis model and primary tumor formation of mouse melanoma. In summary, we identified physiologic factors leading to the control of initial pathways of tumor metastasis and growth.

Materials and methods

Derivation of M1

M1 was prepared according to 'Farmacopeia Homeopática Brasileira'.[16] M1 is composed by the following substances diluted in water, with vigorous shaking in-between dilutions, all together in the same flask: *Aconitum napellus*-20 Hahnemann's dilution (DH), *Arsenicum album*-18 DH, *Asa foetida*-20 DH, *Calcarea carbonica*-16 DH, *Chelidonium majus*-20 DH, *Cinnamon*-20 DH, *Conium maculatum*-17 DH, *Echinacea purpurea*-20 DH, *Gelsemium sempervirens*-20 DH, *Ipecacuanha*-13 DH, *Phosphorus* 20 DH, *Rhus toxicodendron*-17 DH, *Silicea*-20 DH, *Sulfur*-24 DH, and *Thuja occidentalis*-19DH, as previously described.[12]

Mice and cell line

C57BL/6 mice, 7−10 weeks of age (n = 69), were used in experiments according to the approval of the local ethics committee, which certified the procedures using mice in this study are in agreement with the Experimental Animal Brazilian Council and Canadian Council on Animal Care (CEUA certification no 653). Experiments were conducted using pool of mice of equal sex. B16F10 melanoma cell line, purchased from Rio de Janeiro Cell Bank (Rio de Janeiro, Brasil), was cultivated in Dulbecco's Modified Eagle Medium (DMEM) (Sigma−Aldrich) supplemented with 10% heat inactivated fetal bovine serum (FBS) (Invitrogen) at 37°C with 5% CO_2. Cultures were sub-cultivated in strict accordance to the provided instructions and previous report.[17] Briefly, when the confluence neared 90%, cells were detached with 0.05% trypsin − 0.53 mM ethylenediamine tetraacetic acid (EDTA) (Sigma−Aldrich) for 5 min at 37°C; cellular suspension was subsequently diluted at a ratio of 1:10 for culture breeding. For each experiment a new vial of equivalent passage of cryopreserved B16F10 cells was thawed to minimize experimental variation.

Experimental pulmonary metastasis model

B16F10 melanoma cells were detached at 90% confluence as indicated above and resuspended in DMEM with 10% FBS followed by 3 consecutive washes with serum free DMEM. Cell viability was checked with 0.4% trypan blue (Sigma−Aldrich) and standardized at minimal of 90% viability for experimental follow up. After number adjustment by hemocytometer count, detached cells were maintained on ice for no more than 40 min prior injection. C57BL/6 mice were intravenously injected with 5×10^5 B16F10 melanoma cells via the tail vein. 24 h post-injection mice were treated with either M1 or its respective vehicle (ultra-pure water). Solutions were vigorously homogenized and immediate applied to animals via oral inhalation as previously described.[15] Briefly, animals were placed into oral inhalation chambers and treated for 10 min, twice a day, 12 h apart for a period of 14 days. Following 15 days of cell inoculation, mice were anesthetized with 100 mg/kg ketamine (Dopalen−Vetbrands) and 20 mg/kg xilazin (Anasedan−Vetbrands) followed by euthanasia by cervical dislocation. Lungs were subsequently perfused with phosphate buffered 0.9% NaCl solution (PBS) Metastasis foci in the entire lung surface was counted under a stereomicroscope and recorded for each mouse. Subsequently, lungs were analyzed either via: 1)

cells preparation for flow cytometry, 2) histology, or 3) analysis of induced interstitial fluid.

Subcutaneous tumor growth model

B16F10 cells were detached following trypsin-EDTA treatment as described previously and resuspended in DMEM with 10% FBS. Cells were washed twice in PBS and placed in serum free DMEM. Cellular viability was determined by staining cells in 0.4% trypan blue followed by hemocytometer counts. 5×10^5 live cells were subcutaneously injected on dorsal flank of each mouse. 24 h post B16F10 injection, M1 treatment was performed as for the metastasis model. Following 14 days of treatment, mice were euthanized and tumors were removed. Tumors were subsequently weighted, imaged, and processed for histology.

Flow cytometry

Cells from mouse lungs with melanoma were prepared for flow cytometry as previously reported.[17] In brief, the left atrium of euthanized mice was immediately cut and perfused with PBS via the right ventricle to drain peripheral blood from the lungs. Lungs were then surgically excised and processed to achieve homogenization. A scalpel was used to cut lung fragments in pieces ~2 mm in diameter. The fine pieces were then added to an enzyme cocktail in PBS containing 1 mg/ml type IV collagenase (Gibco) and 2U DNase (Ambion), for 45 min at 37°C. Digested lung tissue was passed through a filter with pores of 100 μm diameter (BD Biosciences) and washed in PBS. In this regard, single cell suspensions were generated as previously described.[17] Cell suspensions were subsequently incubated with anti-CD16/32 (clone 2.4G2 − BD Biosciences) for 10 min at 4°C. The following antibodies were subsequently used: anti-CD11b phycoerythrin (PE)-conjugated (clone M1/70 − BD Biosciences), Gr-1-biotinylated (clone RB6-8C5 − BD Biosciences), AT1R (rabbit polyclonal − Santa Cruz Biotechnology), rabbit IgG allophycocyanin-conjugated (Molecular Probes), CD4 PE-conjugated (clone RM4-5 − BD Biosciences), CD8a PE-conjugated (clone 53-6.7 − BD Biosciences), CD45 fluorescein (FITC)-conjugated (clone 30-F11 − BD Biosciences), CD19 PE-conjugated (clone 1D3 − BD Biosciences), NK1.1 PE-conjugated (clone PK136 − Biolegend), CD3 FITC-conjugated (clone 17A2 − BD Biosciences), and FITC-conjugated streptavidin (Vector Laboratories). Primary antibodies were incubated for 40 min at 4°C in PBS with 0.5% FBS; secondary antibodies and streptavidin were incubated for 20 min at 4°C in PBS. Lastly, cells were washed in PBS and immediately acquired in a FACScalibur (BD Biosciences). The cytometry data were post-analyzed using FlowJo vX.0.6 (Tree Star).

Analysis of induced interstitial fluid

Following perfusion, lungs were excised, minced finely and incubated in PBS for 2 h at 37°C, as previously described.[17] The supernatants were separated and processed for cytokines and chemokines analysis using the Cytometric Bead Array Mouse Inflammation Kit (BD Biosciences), according to manual instructions. Samples were acquired in a FACScalibur (BD Biosciences) and post-analyzed using FCAP Array Software (BD Biosciences).

Histology

Lungs and subcutaneous melanoma tumors obtained from mice with melanoma were fixed in 4% paraformaldehyde (Electron Microscopy Sciences) and conventionally processed for histology using Fontana-Masson[18] and Hematoxylin-Eosin[19] staining. For immunohistochemistry and immunofluorescence techniques the following antibodies were used: Ki-67 (clone SP6 − Biocare Medical), Beta-catenin (rabbit polyclonal − EMD Millipore), active caspase-3 (rabbit polyclonal − Biocare Medical), P-Selectin (goat polyclonal − Santa Cruz Biotechnology), and a biotinylated probe for Hyaluronic Acid. Probes were a kind gift of Doctor Helena Nader (Universidade Federal de São Paulo, São Paulo, Brasil), who produces in strict accordance with the previously described method.[18] Nonspecific biding was blocked by incubation with 1% bovine serum albumin (BSA) in PBS for 10 min prior to antibodies staining. Incubations were conducted overnight at 4°C. Immunohistochemistry revelations were performed with the phosphatase/fast red system (catalog number MRCT523G, H, L − Biocare Medical) or the 3,3″-diaminobenzidine tetrahydrochloride (DAB) Substrate Kit (BD Pharmigen™) and further stained with hematoxylin or fast green. Immunofluorescences were revealed with biotinylated antibody coupled to fluorescently tagged streptavidin (anti-mouse/rabbit IgG, cat# BA-1400; anti-goat IgG, cat# BA-9500; fluorescein or texas red fluorescent streptavidin, cat# SA-1200 − Vector Laboratories) in strict accordance with the supplied data sheet. Cellular nuclei were stained with 4′,6-diamidino-2-phenylindole (DAPI − Molecular Probes).Sections were then covered with glass cover slips and mounted using Vectashield (catalog number H-1200 − Vector Laboratories) according to the manufacturer's instructions. Slides were acquired on a slide scanning system (Carl Zeiss Imager Z.2) and analyzed at ImageJ software using the 'Red, Green, and Blue Stack' tool, followed by threshold of the regions of interests, as previously described.[15]

Statistical analysis

Statistical analysis was performed using Graph Pad Prism 6. Two tail unpaired Student's t test was used for the statistical analysis between groups. Values of $p < 0.05$ were considered significant. Data are shown as mean + standard deviation and are representative of at least two independent experiments. No outlier was removed.

Results

Experimental pulmonary metastases and primary tumor growth of melanoma are reduced by M1 treatment

To date, no data has been collected on the *in vivo* role of the homeopathic medicine called M1. In the present work,

we evaluated the anti-melanoma effects of M1 utilizing two models: 1) experimental metastasis; and 2) subcutaneous growth. All mice in these experiments developed melanoma. Due to ethic reasons to avoid animal suffering, by determination of the institutional ethic committee mice were culled on day 15 after tumor challenge. To date, untreated and vehicle treated mice had equivalent tumor burden, therefore we standardized to use the term 'control'. On the other hand, the number of metastatic lesions in M1 treated mice was reduced by 39% compared to vehicle treated (control) group (Figure 1A). Furthermore, quantification of metastatic foci based on the black pigment revealed by Fontana-Masson staining showed a 55% reduction on metastasis formation in M1 group compared to control (Figure 1B), corroborating the observational analysis. Since the correlation that the formation of new nodules in a cancer model is evidence of cancer, the size of the nodules remains an important parameter of disease prognosis[20] and were therefore recorded. They can be identified using Hematoxylin-Eosin staining technique identification of cell nuclei, keratohyalin granules, calcified material, and further stains of eosinophilic structures. The metastatic nodules of M1 treated mice were significantly smaller (Figure 1C). In summary, these results show M1 treatment successfully reduced the quantity and size of melanoma metastases in mice lungs.

We also evaluated M1 anti-melanoma effects using a model of primary tumor formation in the subcutaneous tissue. Visual inspection of tumors showed an obvious decrease in tumor size, which was confirmed by weight measurement indicating tumor size to be reduced by 38% (Figure 1D). Importantly, mice body weight on both groups were in average the same, thus demonstrating that tumor size reduction was due to treatment not to variations on animal size (Figure 4A). To acquire more insight in this effect, histology was conducted via Fontana-Masson (Figure 1E) and Hematoxylin-Eosin staining (Figure 1F), which revealed vastly increased tumor necrotic areas and reduced angiogenesis inside tumors of M1 treated mice compared to control (Figure 1F). These tumor necrotic areas are easily identified by uncharacteristic changes in cellular structures (e.g. nucleus and cytoplasm), characteristic of cell death, and were confirmed by negative reaction for PCNA immunohistochemistry staining (Figure 4B). These data suggest M1 acts against melanoma growth.

Histologic analysis of melanoma reveals better prognostic

To gain more insight in the M1 anti-melanoma effects, we next performed histology of metastases and subcutaneous tumors. We tested tumor proliferation by staining for Ki-67, a marker of proliferation ubiquitously used in cancer studies.[21] Notably, pulmonary metastases from M1 treated mice had significantly fewer melanoma cells Ki-67 positives than vehicle treated mice (Figure 2A). It is widely accepted that the Wnt/beta-catenin signaling is associated with decreased cell proliferation, moreover the coexpression of beta-catenin and Ki-67 is inversely proportional.[22] This means that on a per cell basis, an increase in beta-catenin will in turn reduce the proliferation. Considering the observation that M1 treatment resulted in reduced levels of Ki-67 or less proliferation, we expected an increase of beta-catenin levels. Indeed, immunofluorescence staining showed beta-catenin was significantly increased as compared to the control (Figure 2A).We also examined cell death processes by staining for the active form of caspase-3, a protease that triggers programmed cell death.[23] Immunofluorescence indicated a massive induction of active caspase-3 in melanoma cells from M1 treated mice, whereas the control expressed little to none (Figure 2A). We also confirmed these results with the subcutaneous tumors and found it is a conserved phenotype. Ki-67 is also reduced on subcutaneous melanoma tumors from M1 group (Figure 2B). However, despite the obvious trend, we could not detect a statistically confirmed increase in the levels of Beta-Catenin (Figure 2B) and tumor death content by Fontana-Masson staining (Figure 2B).

All these effects are characteristic of tumor starvation due to impaired angiogenesis. Therefore we investigated in the pulmonary metastases the tumor-related angiogenesis by staining vessels with P-Selectin, a protein expressed in endothelial cells and platelets.[24] Interestingly, the quantity of intratumoral P-Selectin$^+$ cells is significantly reduced in the M1 group (Figure 2C). We then investigated the tumor angiogenesis in the subcutaneous tumors. Intratumour vessels formation was detected by immunohistochemistry to a glycosaminoglycan of vascular endothelial cells basal lamina, Hyaluronic Acid.[25] By ImageJ analysis of tumor sections, we counted the total quantity of vessels by representation in 3 groups: smaller than (<) 15 μm, bigger than (>) 15 μm, and total vessels. Total vessel formation was reduced with high significance ($p < 0.01$). Interestingly, vessels bigger than 15 μm were not modified, but we found a significant reduction in the quantity of vessels smaller than 15 μm, the capillaries-like structures (Figure 2D). These results are suggestive that melanoma tumors are suffering of starvation with fewer vessels content by treatment with M1, which promoted reduction in tumor burden. In summary, these results suggest a reduced phenotype of malignancy in the mouse melanoma metastases and subcutaneous tumors by treatment with M1.

Changes in lung cellular content is associated with anti-melanoma effects of M1

Since the immune system plays an important role to the control of tumors,[6] we next aimed to check whether the suppression of melanoma metastasis could be related to an increased immunologic response. To address this question, we analyzed the frequencies of different leukocytes populations in the lungs by flow cytometry, such as macrophages, dendritic cells, NK cells, CD8$^+$ T cells, CD4$^+$ T cells, and B cells, which were identified as CD45.2$^+$ plus double staining CD11b$^+$ F4/80$^+$, CD11c$^+$ F4/80$^-$, NK1.1$^+$ CD3ε^-, CD8a$^+$ CD3ε^+, CD4$^+$ CD3ε^+ or B220$^+$ CD3ε^-, respectively. Strikingly, there were no differences in the frequencies of all these populations (Figure 3A).

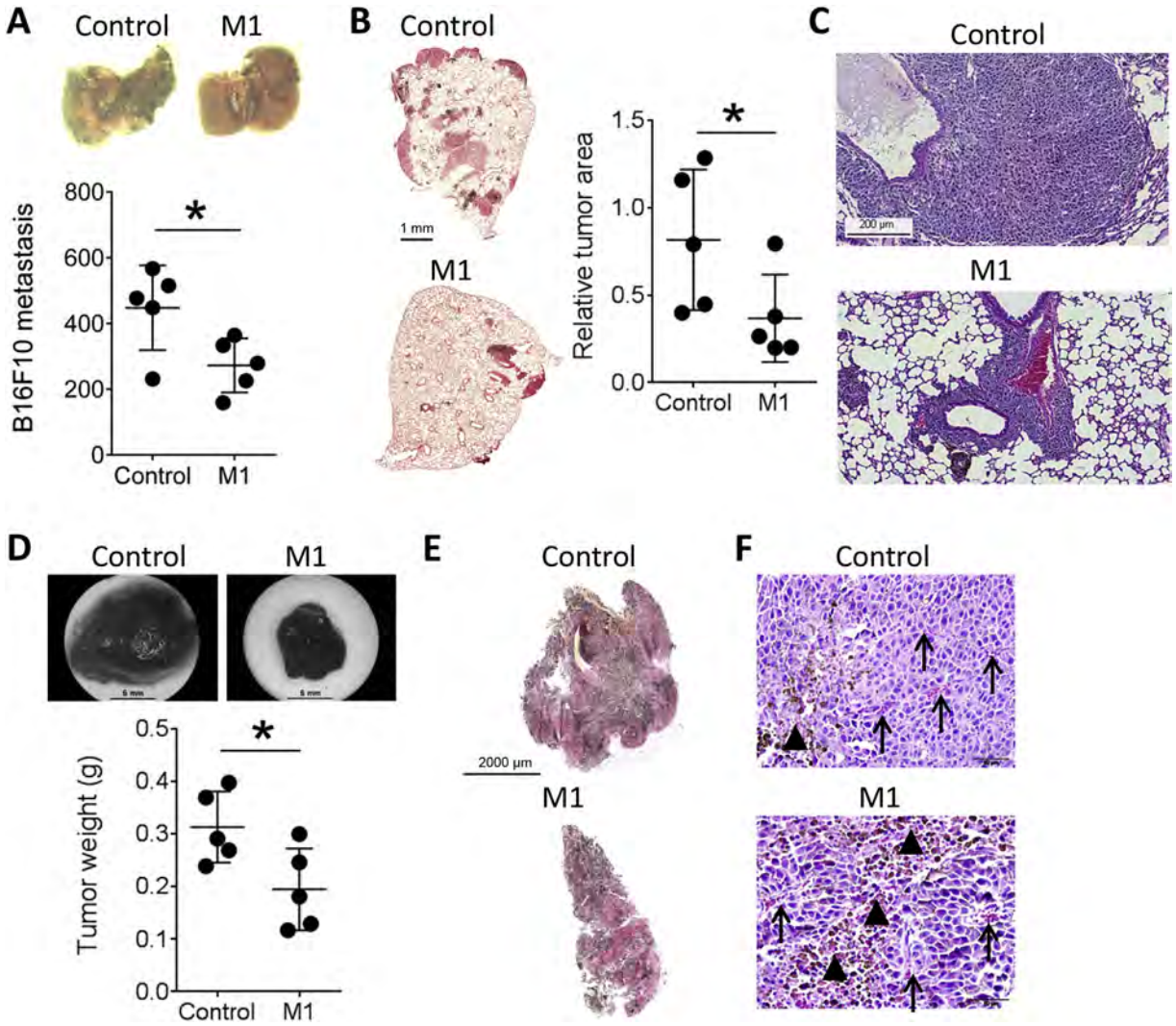

Figure 1 Treatment with M1 reduces melanoma metastases and growth. Mice were injected with 2×10^5 B16F10 melanoma cells i.v. (A–C) or subc. (D–F) and treated with M1 or vehicle from day 1–14 relative to tumor challenge, as described in Material and methods. (A) On day 15, mice injected i.v. were euthanized, lungs removed and quantities of melanoma metastases recorded for each individual mouse. (B) Lungs were processed for Fontana-Masson staining to identify melanoma metastases by histology. In this staining, cell nuclei have the red color while melanin from melanoma metastases is black. Metastases were quantified based on the black staining by software ImageJ. (C) Lungs were processed for Hematoxylin-Eosin staining to compare metastasis sizes. (D) On day 14, mice injected subc. with B16F10 were euthanized, subcutaneous tumors removed, and the weight measured and recorded for each individual tumor. (E) Subcutaneous tumors were processed for Fontana-Masson staining. (F) Tumors stained with Hematoxylin-Eosin to identify 'tumor necrotic areas' (▲) and intratumoral vessels (↑). Data are representative of 2–5 independent experiments. Statistic analysis performed by unpaired Student's t test. *p<0.05. (For interpretation of the references to color in this figure legend, the reader is referred to the web version of this article.)

Since the better understanding of local environmental milieu is important to characterize the immunologic response in the lungs,[17] we assayed for different inflammatory cytokines. For this purpose, Cytometric Bead Array by flow cytometry quantification of IL-10, IL-12p70, Tumor Necrosis Factor (TNF), Monocyte Chemotactic Protein-1 (MCP-1), Interleukin-6 (IL-6) and Interferon-γ (IFN-γ) was performed. Interestingly, IL-10 was upregulated, whereas TNF, MCP-1 and IL-6 were not changed. Detectable amounts of IL-12p70 were only found on the M1 group. IFN-γ could not be detected (Figure 3B). In summary, these results indicate the suppression of melanoma metastases by M1 is not related to changes in the cellular content analyzed from innate and adaptive immunologic responses in the lungs, but significant changes in the cytokine content could be detected. This spirited further investigations, such as of cells recruited by the tumor.

It is known that myeloid derived suppressor cells (MDSC) are recruited by tumor cells to create an immunosuppressive environment. Furthermore, these cells are $CD11b^+$ and can be classified according to the level of Gr-1 expression, such as $Gr\text{-}1^{high}$, $Gr\text{-}1^{intermediate\ (int)}$, and $Gr\text{-}1^{low}$, which have high, intermediate or low expression of Gr-1, respectively.[26] On the other hand, expression of angiotensin II type 1 receptor (AT1R) on tumor-associated macrophages has been associated with increased melanoma growth,[27,28] but this receptor has not yet been shown on MDSC. Therefore we expanded our

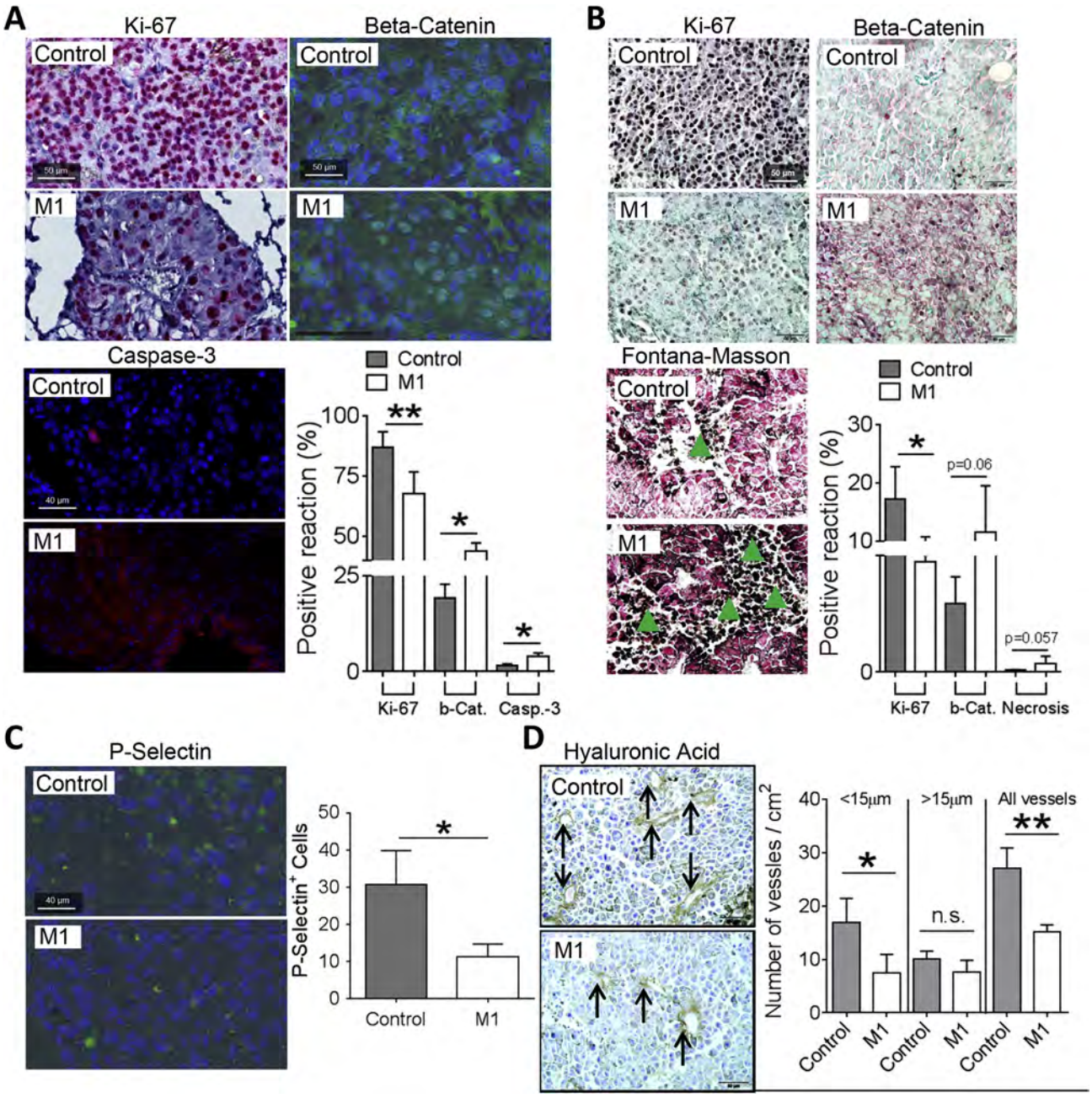

Figure 2 Prognostic marker analysis for metastatic melanoma after treatment with M1. Mice were injected with 2×10^5 B16F10 melanoma cells i.v. (A and C) or subc. (B and D) and treated with M1 or vehicle from day 1−14 relative to tumor challenge, as described in material and methods. (A and C) On day 15, mice were euthanized, lungs removed and processed for different histology techniques and the staining quantified by ImageJ. (B and D) On day 15 subcutaneous tumors were removed following euthanasia and processed for histology with subsequently analysis by ImageJ. (B) Green triangles indicate tumor necrotic areas. (D) The arrows on hyaluronic acid staining indicate the vessels. Data are representative of 2 independent experiments. Statistic analysis performed by unpaired Student's t test. *p < 0.05; **p < 0.01. (For interpretation of the references to color in this figure legend, the reader is referred to the web version of this article.)

analysis to investigate whether such cells express AT1R and whether they are impacted by M1 treatment in the pulmonary environment. Interestingly, M1 treated mice had fewer $CD11b^+$ $Gr\text{-}1^{low}$ cells in the lungs with melanoma (Figure 3C). Furthermore, these cells have the highest expression of AT1R, which was also reduced in the M1 treated mice (Figure 3D). We also checked for the presence of $AT1R^+$ cells in the subcutaneous melanoma and found to be significantly reduced on tumor periphery (Figure 3E). These results indicate a mechanism of action for the anti-melanoma properties of M1: the control of AT1R expression on intratumoral MDSC, subsequently leading to reduced tumor angiogenesis.

Discussion

Over the past several decades drug discovery has produced significantly advances to cancer therapy; however,

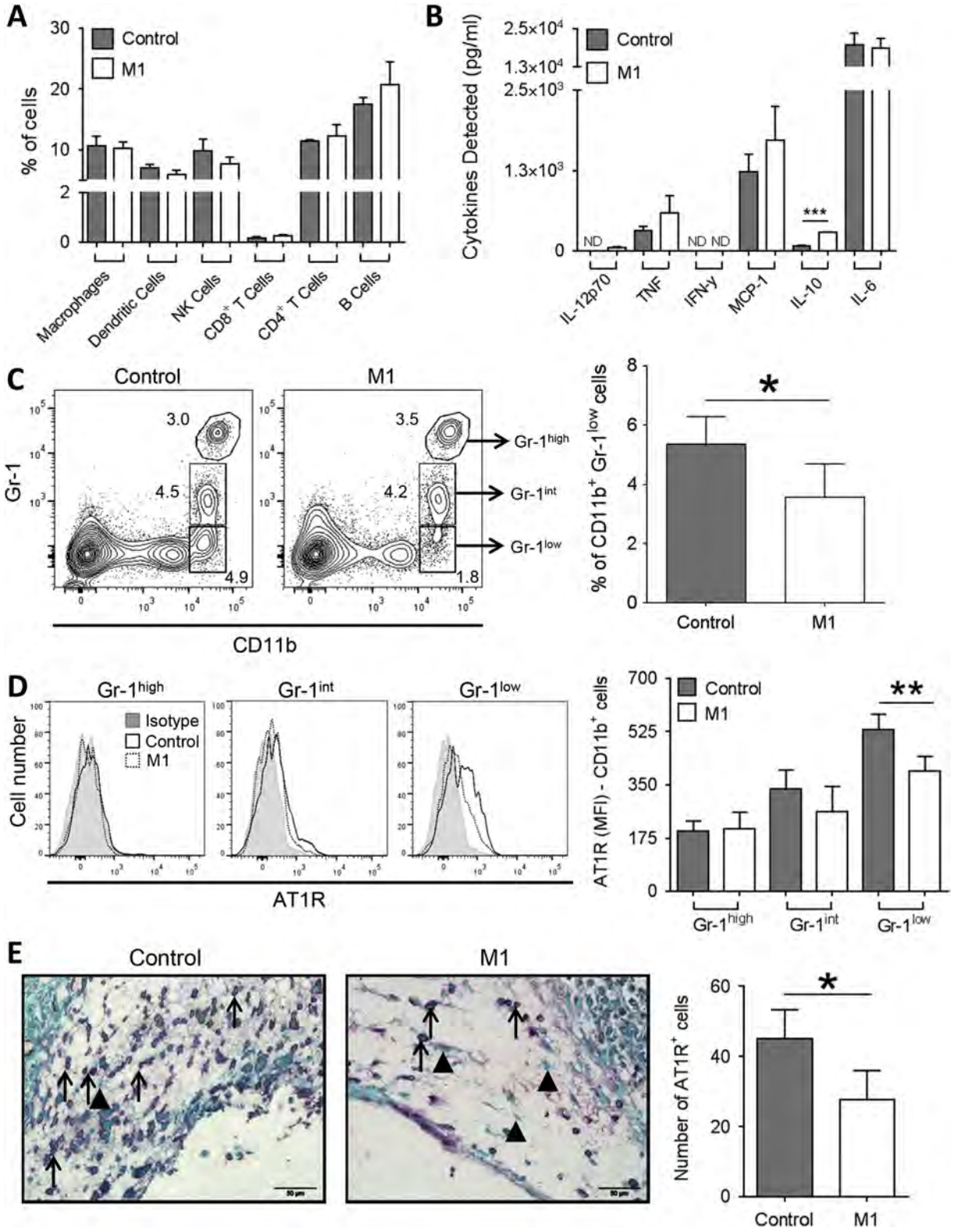

Figure 3 Inhibition of AT1R$^+$ cells is associated with the control of melanoma growth by M1. Mice were injected with 2×10^5 B16F10 melanoma cells i.v. (A–D) or subc. (E) and treated with M1 or vehicle from day 1–14 relative to tumor challenge, as described in material and methods. (A, C and D) On day 15, mice injected i.v. were euthanized, lungs perfused with PBS to remove peripheral blood and processed for FACS. (B) Cytokines content in the interstitial fluid of the lungs was analyzed by CBA and FACS, as described in the material and methods. ND, not detected. (E) Subcutaneous tumors were processed for AT1R immunohistochemistry to identify AT1R+ cells (pink color, indicated by '↑') and negative for this receptor (▲) on tumor periphery and analyzed by ImageJ. Data are representative of 2 independent experiments, each consisting of 5 mice per group. Statistic analysis performed by unpaired Student's t test. *$p < 0.05$; **$p < 0.01$. (For interpretation of the references to color in this figure legend, the reader is referred to the web version of this article.)

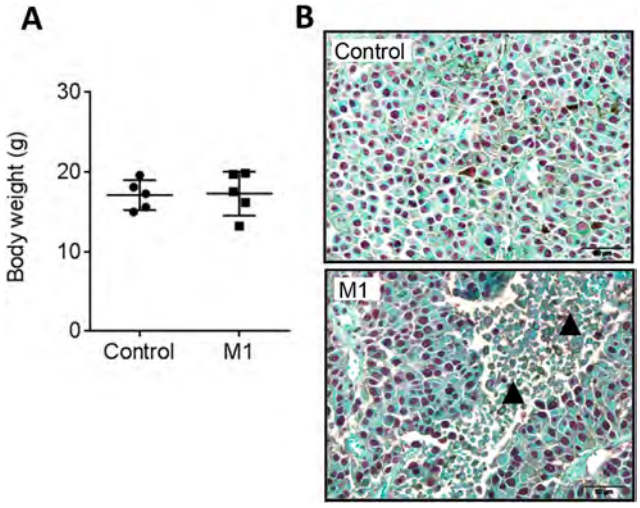

Figure 4 Analysis of mice with subcutaneous B16F10 after treatment with M1. Mice were injected with 2×10^5 B16F10 melanoma cells subc. and treated with M1 from day 1−14 relative to tumor challenge, as described in material and methods. (A) On day 15, just before the euthanasia, the weight of mice were measured and recorded for each individual mouse. (B) Subcutaneous tumors were processed for immunohistochemistry to detect PCNA (pink color). Fast green was used as counterstainer. Data are representative of 2 independent experiments consisting of 5 mice per group. Statistic analysis performed by unpaired Student's t test. (For interpretation of the references to color in this figure legend, the reader is referred to the web version of this article.)

metastatic melanoma remains an incurable disease. To address this problem, our research group has been systematically evaluating medicines that have already been shown to produce target effects against *in vitro* cancer models.[12] Considering the importance of drug discovery or the implications that could be derived from novel properties of new compounds, we tested M1, a commercial homeopathic medicine used as complementary therapy for cancer, in an experimental mouse model for the skin cancer melanoma. Here, we observed several indications demonstrative of a successfully formulation in the treatment of melanoma: 1) mice treated with M1 have reduced both melanoma metastases and primary tumor formation; 2) tumors of M1 treated mice have reduced angiogenesis and proliferation, while higher levels of tumor death and beta-catenin, which are 'good' prognostic markers; and 3) fewer frequency of the tumor associated MDSC characterized by the markers CD11/Gr-1 in addition to lower expression of AT1R in these cells. In summary, these results suggest treatment with M1 is efficient for melanoma therapy.

It is known that the number of pulmonary metastasis in mice that were tail vein injected with tumors cells, like melanoma, directly correlates to the malignancy of a cell line and the effectiveness of an anti-neoplastic drug.[29] Here tumor burden was evaluated by quantifying the frequency of metastatic lesions. Despite this parameter provide robustness and reproducibility, using ImageJ's analysis of Fontana-Masson and Hematoxylin-Eosin staining we were able to measure metastatic colony formation, frequency, and size by microscopy, adding much needed parameters to properly assay cancer progression. Surprisingly, these parameters permitted not only the observation of metastasis quantity reduction, but also tumor sizes in the lungs. Furthermore, the subcutaneous tumor model provided insights for the effects of M1 against melanoma growth. Therefore these data increased our interest in factors leading to both tumor metastasis and growth.

MDSC is a population of host immune cells producers of immunosuppressive factors that play an important role for tumor immune evasion mechanisms.[30] Interestingly, the accumulation of these cells is associated with tumor growth.[31] Therefore MDSC represent an interesting target to block immune suppression and trigger antitumor response, which can improve the outcome of current therapies, as has been shown before.[32] Here we showed the population of MDSC $CD11b^+$ $Gr\text{-}1^{low}$ is significantly less present in the lungs of mice treated with M1 after B16F10 injection, which would suggest a less immunosuppressed microenvironment. However, we could not detected differences in the frequencies of immune cells with anti-tumor potential, such as NK cells and CD8 T cells, nor differences strong enough to be considered biologically relevant on cytokines production. On the other hand, AT1R expression on $CD11b^+$ $Gr\text{-}1^{low}$ cells is significantly reduced by M1 treatment. This receptor is one of the two receptor subtypes for the key biological peptide Angiotensin II which regulates blood pressure and renal hemodynamics, acting as a principle regulator of cardiovascular homeostasis.[33] Surprisingly, AT1R blockade results in growth inhibition of a pancreatic cancer cell line[34] and AT1R antagonists resulted in the prevention of pulmonary cancer by inhibition of tumor angiogenesis.[35] Furthermore, this receptor is also frequently expressed in *in vivo* cancers such as renal cancer,[35] human endometrial cancer,[36] mouse fibrosarcoma cancer,[37] rat glioma[38] and mouse melanoma.[39] Using the conception that AT1R antagonists will reduce tumor burden, as further substantiated by $AT1R^{-/-}$ mice in which decreased tumor growth rates and a reduction of blood vessels was observed,[28] the reduction of AT1R expression on $CD11b^+$ $Gr\text{-}1^{low}$ cells after treatment suggests the mechanism by which pulmonary metastasis and primary tumor growth are suppressed by M1. Importantly, this is the first study that reports the presence of AT1R on MDSC, which promotes the hypothesis of a novel function yet to be described in tumor biology: the production of chemotactic factors to initiated vessel formation. Despite providing a clue that AT1R expression on MDSC regulates cancer progress, more extensive examination is needed to provide this statement with higher degree of confidence.

Up until this point we observed many indicators that tumor suppression was driven by a lacking blood supply: smaller metastasis size, fewer tumor-related angiogenesis, Ki-67 reduction and increased caspase-3 activation. These events can be considered consequences of inhibition of tumor angiogenesis, instead of a direct action of M1 on

melanoma cells. We speculate therefore that the reduction in cellular proliferation, increased caspase-3 activation and higher beta-catenin content are contributing factors to the decreased size and frequency of tumor nodules in M1 treated mice due to modulation of angiogenesis. Altogether these results indicate treatment with M1 prevents a critical phase of metastasis establishment by limiting tumor-related angiogenesis, which is a very promising result considering clinically approved anticancer medicines such as Bevacizumab and Sorafenib in which blockade of angiogenesis has similar characteristics of cancer reduction.[40]

Conclusions

Here we have reported M1's ability to produce anti-melanoma effects in mice. We identified a potential mechanism of action through the modulation of frequency and expression of AT1R on MDSC. The anticancer role of M1 in melanoma demonstrates M1 is effective as a host immunity modulator. Additionally, considering the highly diluted properties M1 offers an advantage to provide a cost effective alternative to costly chemotherapeutic approaches with, if any, lower toxicity.

Conflict of interests statement

The authors declare they have no competing interests.

Authors' contributions

LFA carried out all the experiments, analyzed the data and wrote manuscript. ARL, GR, CRVC, RZ, and FSFG carried out some of the experiments involving mouse work. BM, EST and CCO revised the manuscript. DFB designed the project.

Acknowledgments

This work was supported by grants from 'Fundação Araucária' (grant no 18797) and scholarships from 'Coordenação de Aperfeiçoamento de Pessoal de Nível Superior', 'Conselho Nacional de Desenvolvimento Científico e Tecnológico' and 'Pró-Reitoria de Extensão e Cultura da Universidade Federal do Paraná'. The funding source had not involvement in study design, collection, analysis or interpretation of data.

References

1 *GLOBOCAN*. IARC, 2012.
2 Siegel R, Ma J, Zou Z, Jemal A. Cancer statistics. *CA Cancer J Clin* 2014; **2014**(64): 9–29.
3 Houghton AN, Polsky D. Focus on melanoma. *Cancer Cell* 2002; **2**: 275–278.
4 Finn L, Markovic SN, Joseph RW. Therapy for metastatic melanoma: the past, present, and future. *BMC Med* 2012; **10**: 23.
5 Sapoznik S, Hammer O, Ortenberg R, *et al*. Novel anti-melanoma immunotherapies: disarming tumor escape mechanisms. *Clin Dev Immunol* 2012; **2012**: 818214.
6 Vesely MD, Kershaw MH, Schreiber RD, Smyth MJ. Natural innate and adaptive immunity to cancer. *Annu Rev Immunol* 2011; **29**: 235–271.
7 Schaer D, Lesokhin M, Wolchok JD. Hiding the road signs that lead to tumor immunity. *J Exp Med* 2011; **208**: 1937–1940.
8 De Oliveira SM, de Oliveira CC, Abud APR, *et al*. Mercurius solubilis: actions on macrophages. *Homeopathy* 2011; **100**: 228–236.
9 Cesar B, Abud APR, De Oliveira CC, *et al*. Treatment with at homeopathic complex medication modulates mononuclear bone marrow cell differentiation. *Evid Based Complement Alternat Med* 2011; **2011**.
10 Guimarães FSF, Abud APR, Oliveira SM, *et al*. Stimulation of lymphocyte anti-melanoma activity by co-cultured macrophages activated by complex homeopathic medication. *BMC Cancer* 2009; **9**: 293.
11 Sato D, Wal R, De Oliveira C, *et al*. Histopathological and immunophenotyping studies on normal and sarcoma 180-bearing mice treated with a complex homeopathic medication. *Homeopathy* 2005; **94**: 26–32.
12 Oliveira CC, Abud APR, de Oliveira SM, *et al*. Developments on drug discovery and on new therapeutics: highly diluted tinctures act as biological response modifiers. *BMC Complement Altern Med* 2011; **11**: 101.
13 Molassiotis A, Fernadez-Ortega P, Pud D, *et al*. Use of complementary and alternative medicine in cancer patients: a European survey. *Ann Oncol* 2005; **16**: 655–663.
14 Ott P, Hodi FS, Robert C. CTLA-4 and PD-1/PD-L1 blockade: new immunotherapeutic modalities with durable clinical benefit in melanoma patients. *Clin Cancer Res* 2013; **19**: 5300–5309.
15 Guimarães FSF, Andrade LF, Martins ST, *et al*. In vitro and in vivo anticancer properties of a *Calcarea carbonica* derivative complex (M8) treatment in a murine melanoma model. *BMC Cancer* 2010; **10**: 113.
16 *Brasil. Farmacopeia Homeopática Brasileira*, 3th edn, Comissão da Farmacopeia Brasileira, 2011, 1–364.
17 Chow MT, Sceneay J, Paget C, *et al*. NLRP3 suppresses NK cell-mediated responses to carcinogen-induced tumors and metastases. *Cancer Res* 2012; **72**: 5721–5732.
18 Bishop J, Nelson AM, Merz WG, Askin FB, Riedel S. Evaluation of the detection of melanin by the Fontana-Masson silver stain in tissue with a wide range of organisms including Cryptococcus. *Hum Pathol* 2012; **43**: 898–903.
19 Avwioro G. Histochemical uses of haematoxylin – a review**1**(-June): 24–34.
20 Nakamura K, Yoshikawa N, Yamaguchi Y, Kagota S, Shinozuka K, Kunitomo M. Characterization of mouse melanoma cell lines by their mortal malignancy using an experimental metastatic model. *Life Sci* 2002; **70**: 791–798.
21 De Andrade BAB, León JE, Carlos R, Delgado-Azañero W, Mosqueda-Taylor A, de Almeida OP. Expression of minichromosome maintenance 2, Ki-67, and geminin in oral nevi and melanoma. *Ann Diagn Pathol* 2013; **17**: 32–36.
22 Chien AJ, Moore EC, Lonsdorf AS, *et al*. Activated Wnt/beta-catenin signaling in melanoma is associated with decreased proliferation in patient tumors and a murine melanoma model. *Proc Natl Acad Sci U S A* 2009; **106**: 1193–1198.
23 Snigdha S, Smith ED, Prieto GA, Cotman CW. Caspase-3 activation as a bifurcation point between plasticity and cell death. *Neurosci Bull* 2012; **28**: 14–24.
24 Stevens T. Functional and molecular heterogeneity of pulmonary endothelial cells. *Proc Am Thorac Soc* 2011; **8**: 453–457.
25 Lennon FE, Singleton PA. Hyaluronan regulation of vascular integrity. *Am J Cardiovasc Dis* 2011; **1**: 200–213.
26 Dolcetti L, Peranzoni E, Ugel S, *et al*. Hierarchy of immunosuppressive strength among myeloid-derived suppressor cell subsets is determined by GM-CSF. *Eur J Immunol* 2010; **40**: 22–35.

27 Cortez-Retamozo V, Etzrodt M, Newton A, *et al*. Angiotensin II drives the production of tumor-promoting macrophages. *Immunity* 2013; **38**: 296−308.
28 Egami K, Murohara T, Shimada T, *et al*. Role of host angiotensin II type 1 receptor in tumor angiogenesis and growth**112**: 67−75.
29 Welch DR. Technical considerations for studying cancer metastasis in vivo**15**: 272−306.
30 Youn J-I, Nagaraj S, Collazo M, Gabrilovich DI. Subsets of myeloid-derived suppressor cells in tumor-bearing mice. *J Immunol* 2008; **181**: 5791−5802.
31 Bunt SK, Yang L, Sinha P, Clements VK, Leips J, Ostrand-Rosenberg S. Reduced inflammation in the tumor microenvironment delays the accumulation of myeloid-derived suppressor cells and limits tumor progression. *Cancer Res* 2007; **67**: 10019−10026.
32 Schilling B, Sucker A, Griewank K, *et al*. Vemurafenib reverses immunosuppression by myeloid derived suppressor cells. *Int J cancer* 2013; **133**: 1653−1663.
33 Cuadra AE, Shan Z, Sumners C, Raizada MK. A current view of brain renin-angiotensin system: is the (pro)renin receptor the missing link? *Pharmacol Ther* 2010; **125**: 27−38.
34 Fujimoto Y, Sasaki T, Tsuchida A, Chayama K. Angiotensin II type 1 receptor expression in human pancreatic cancer and growth inhibition by angiotensin II type 1 receptor antagonist. *FEBS Lett* 2001.
35 Miyajima A, Kosaka T, Asano T, Asano T, Seta K, Kawai T. Angiotensin II type I antagonist prevents pulmonary metastasis of murine renal cancer by inhibiting tumor angiogenesis advances in brief angiotensin II type I antagonist prevents pulmonary metastasis of murine renal cancer by inhibiting tumor angiogenesis. *Cancer* 2002; **62**: 4176−4179.
36 Choi CH, Park Y-A, Choi J-J. Angiotensin II type I receptor and miR-155 in endometrial cancers: synergistic antiproliferative effects of anti-miR-155 and losartan on endometrial cancer cells. *Gynecol Oncol* 2012;1−8.
37 Fujita M, Hayashi I, Yamashina S, Itoman M, Majima M. Blockade of angiotensin AT1a receptor signaling reduces tumor growth, angiogenesis, and metastasis. *Biochem Biophys Res Commun* 2002; **294**: 441−447.
38 Arrieta O, Guevara P, Escobar E, García-Navarrete R, Pineda B, Sotelo J. Blockage of angiotensin II type I receptor decreases the synthesis of growth factors and induces apoptosis in C6 cultured cells and C6 rat glioma. *Br J Cancer* 2005; **92**: 1247−1252.
39 Otake AH, Mattar AL, Freitas HC. Inhibition of angiotensin II receptor 1 limits tumor-associated angiogenesis and attenuates growth of murine melanoma. *Cancer Chemother Pharmacol* 2010; **66**: 79−87.
40 Zaki KA, Basu B, Corrie P. The role of angiogenesis inhibitors in the management of melanoma. *Curr Top Med Chem* 2012; **12**: 32−49.